# Epitope-independent purification of native-like envelope trimers from diverse HIV-1 isolates

**Running Title:** Epitope-independent SOSIP purification

Hans P. Verkerke[1], James A. Williams[1], Miklos Guttman[1], Cassandra A. Simonich[2], Yu Liang[1], Modestas Filipavicius[1], Shiu-Lok Hu[3], Julie Overbaugh[2], Kelly K. Lee[1,*]

[1] Department of Medicinal Chemistry, University of Washington, Seattle, WA 98102, USA

[2] Division of Human Biology, Fred Hutchinson Cancer Research Center, Seattle, WA 98102, USA

[3]Department of Pharmaceutics and Washington National Primate Research Center

[*]Address correspondence to: kklee@uw.edu

## ABSTRACT

Soluble forms of trimeric HIV-1 envelope glycoprotein (Env) have long been sought as immunogens and as reagents for analysis of Env structure and function. Isolation of trimers that mimic native Env, derived from diverse viruses, however, represents a major challenge. Thus far, the most promising "native-like" (NL) structures have been obtained by engineering trimer-stabilizing mutations, termed "SOSIP," into truncated Env sequences. However, the abundance of NL trimeric conformers varies among Envs, necessitating purification by monoclonal antibodies (Mabs) like PGT145, which target specific epitopes. To surmount this inherent limitation, we developed an approach that uses lectin affinity, ion exchange, hydrophobic interaction, and size exclusion chromatography to isolate NL trimers from non-native Env species. We validated this method with SOSIP trimers from HIV-1 clades A and B. Analyses by SEC, blue native- and SDS-PAGE, and dynamic light scattering indicated that the resulting material was homogeneous (>95% pure), fully-cleaved, and of the appropriate molecular weight and size for SOSIP trimers. Negative stain-electron microscopy further demonstrated that our preparations were composed of NL trimeric structures. By hydrogen/deuterium-exchange mass spectrometry, these HIC-pure trimers exhibited structural organization consistent with NL trimers and inconsistent with profiles seen in non-native Envs. Screened for antigenicity, some Envs like BS208.b1 and KNH1144 T162A, did not present the glycan/quaternary structure-dependent epitope for PGT145 binding, suggesting that these SOSIPs would be challenging to isolate by existing Mab affinity methods. By selecting based on biochemical rather than antigenic properties, our method offers an epitope-independent alternative to Mabs for isolation of NL Env trimers.

**IMPORTANCE**

The production and purification of diverse soluble Env trimers that maintain native-like (NL) structure present technical challenges that must be overcome in order to advance vaccine development and provide reagents for HIV research. Low levels of NL trimer expression amid heteroeneous Env conformers, even with the addition of stabilizing mutations, has presented a major challenge. In addition, it has been difficult to separate the NL trimers from these heterogeneous mixtures. While Mabs with specificity for quaternary NL trimer epitopes have provided one approach to purifying the desirable species, such methods are dependent on the Env displaying the proper epitope. In addition, Mab affinity chromatography can be expensive, the necessary Mab may be in limited supply, and large-scale purification may not be feasible. Our method based on biochemical separation techniques offers an epitope-independent approach to purification of NL trimers with general application to diverse Envs.

## INTRODUCTION

The envelope glycoprotein (Env) on the virus surface is the sole target of HIV-1 neutralizing antibodies (Nabs). Many vaccine strategies involve the use of Env-based immunogens aimed at eliciting Nabs with broad cross-reactivity. Because the trimeric form of Env found on the surface of the virus mediates viral entry, and a major goal of vaccine design is to elicit antibodies that block this process, it is expected that immunogens must recapitulate the native structure of this functional Env (1–6). Diverse Env variants representing the most prevalent HIV-1 clades are currently under evaluation as potential immunogens.

Functional Env is a membrane-anchored trimer of extensively glycosylated heterodimers, composed of gp120 receptor binding and gp41 membrane spanning fusion subunits. Endogenous proteases cleave the gp160 precursor polypeptide into gp120 and gp41 subunits, which remain non-covalently associated as protomers in the native Env trimer. Current models of viral entry suggest that, prior to receptor and co-receptor binding, Env adopts a “closed” pre-fusion conformation, in which conserved functional features such as receptor and co-receptor binding sites on the gp120 core and the V3 loop are “masked” or sterically inaccessible (7, 8). Dense clusters of N-linked glycans distributed across the surface of Env as well as on its flexible variable loops further shield conserved core features (9, 10). Despite the significant defenses that have evolved on Env to mask the conserved features, recent studies have demonstrated that broadly neutralizing antibodies (BNabs) can target select epitopes distributed across much of the surface of the closed, prefusion form of Env (11).

As a Type 1 fusion protein, in which the prefusion conformation exists as a high-energy, metastable state, Env is relatively prone to spontaneous transition to its post-fusion state (12–14). It is believed that Env may have been additionally selected for a tendency to misfold, possibly as a mechanism of immune evasion, whereby immunodominant but non-native, non-functional forms of Env are displayed on the virus surface alongside relatively few copies of functional, native trimer (15). As a consequence of these and other factors, early efforts to produce soluble, recombinant forms of Env glycoproteins were largely unsuccessful (16). First

89 generation uncleaved gp140 ectodomain constructs, which truncated the Env gene N-terminal
90 to the transmembrane anchor, were found to be lack native-like (NL) Env structural organization
91 (16, 17). Such engineered proteins, derived from a range of Env sequences, in general
92 appeared to adopt non-native conformations in which the gp41 subunit degenerates to a highly
93 stable, helical bundle state, resembling the post-fusion conformation, while gp120 monomers
94 remain loosely tethered or dissociated with disordered V1/V2 and V3 loops (16, 17). As a
95 consequence, uncleaved gp140s expose epitopes targeted by poorly neutralizing antibodies
96 that are occluded on the native trimer (18). When used in vaccines, they are thus unlikely to
97 elicit broadly neutralizing humoral responses that target the NL, closed prefusion trimer
98 organization (18–21).

99 In order to overcome the limitations of this first generation of Env constructs, much of the
100 recent focus of Env immunogen design has been on producing stabilized forms of trimeric Env
101 that maintain the structural and antigenic features of the native closed pre-fusion conformation.
102 A set of modifications to the Env sequence were identified that help reduce formation of non-
103 native Env proteins while enhancing formation of NL trimers (22–25). These modifications, when
104 paired with selection of Env from specific viral variants that favor NL trimer formation, resulted in
105 production of trimeric glycoprotein assemblies that closely resemble native Env trimers (26–30)
106 and have led to breakthroughs in structure determination, which in turn identified additional
107 stabilizing substitutions that lock the assembly in the closed, prefusion conformation (4, 31).

108 The most widespread approach to date for generating stabilized NL Env trimers employs
109 “SOSIP.v1” modifications (4, 26). In this approach, Env is truncated after residue 664 and thus
110 lacks both the transmembrane and membrane proximal domains of gp41; an Ile to Pro
111 replacement is introduced in the first heptad repeat of the ectodomain of gp41 ($gp41_{ecto}$),
112 stabilizing the pre-fusion state; an engineered disulfide bridge links $gp41_{ecto}$ and gp120 subunits
113 of each protomer to prevent their dissociation; and a hexa-arginine motif replaces the native
114 cleavage sequence to enhance furin cleavage. Despite these modifications potentially altering
115 some structural properties, this design and those based on it represent the most native-like

reagent available for the study of Env using solution based techniques. Purified, trimeric SOSIP.v1 Envs have been shown by numerous structural and biophysical techniques to faithfully mimic HIV-1 Env (27, 32–34) in its native, trimeric conformation (26). Furthermore, a SOSIP.v1 trimer engineered from the Env sequence of the transmitted form of the virus from an infant in the Nairobi Breastfeeding Clinical Trial (NBT), BG505.c2 T332N (35), effectively elicited potent neutralizing antibodies in rabbits and macaques (36). However, these Nabs lacked broad cross-reactivity—meaning that they failed to neutralize heterologous tier-2 and 3 viruses. It has therefore been proposed that elicitation of broadly neutralizing responses may require the use of polyvalent formulations of SOSIP Envs based on diverse viral variants to accomplish the hallmark goal of breadth and potency. Env from different isolates, however, vary widely in their propensities to form recombinant NL trimers using the SOSIP design (37, 38). Consequently, numerous purification methods have been developed to isolate NL trimers from lower yield Envs.

Positive selection of glycosylated proteins by affinity chromatography with lectins or glycan dependent Nabs like 2G12 followed by gel filtration is a commonly employed method of SOSIP protein purification (35). While these steps provide some separation of Env species, such methods alone are not sufficient to isolate NL trimer from misfolded dimers and other non-native conformations. A more stringent form of positive selection employs quaternary structure-dependent monoclonal antibodies PGT145 (37) and PGT151 (38). These approaches, based on selection of complexes that present the cognate epitope for the Mab employed, have proven effective and generalizable to SOSIP trimers designed from several isolates. An alternative, affinity based method uses negative selection with antibodies such as F105 and GE1366 (39), which are directed toward epitopes that are exposed on dimeric and monomeric species, but are occluded on the “closed” properly folded NL trimer. While such affinity methods have proven effective in purifying NL trimers designed from some isolates, they require the antigen to present specific protein and glycan epitopes that are not necessarily universal to isolates of interest. In

most cases, the required antibodies are not widely available, and it also remains relatively cost-prohibitive to scale Mab-purification as may be needed for vaccine production.

To circumvent the limitations of Mab affinity methods for SOSIP purification, we developed an approach that relies on biochemical rather than antigenic features of well-formed NL SOSIP trimer and applied it to the purification of SOSIP.v1 trimers based on diverse Env sequences. The method we describe is effective in isolating the NL trimer population even when it is a minority fraction of the total Env material. By making it possible to isolate a broad range of NL Env trimers and use them as reagents (e.g. for antigenicity assays, B cell sorts, and structural analyses), we anticipate that it will become possible to investigate the diversity of HIV-1 Env biology and Env-directed immune responses with greater rigor and scope than in the past. Since the approach we describe relies upon readily scalable biochemical methods, this and similar purification methods are expected to be amenable to production of large-scale preparations, which may be useful for vaccine production.

## MATERIALS AND METHODS

### Design of SOSIPs engineered from multiple HIV-1 envelope sequences.

The amino acid sequence of the canonical BG505.c2 SOSIP.664 T332N was used as a template for design of new SOSIP.664 constructs engineered from gp160 sequences of diverse HIV-1 isolates. Briefly, a disulfide bridge was introduced between cysteines at positions 501 and 605 (SOS) and an Ile-to-Pro mutation was introduced in the HR1 domain of gp41 (IP). We also modified the native proteolytic cleavage site $_{508}$REKR$_{511}$ to a hexa-arginine motif, known to enhance cleavage by exogenous furin (26), and replaced the native leader sequence with that of the tissue plasminogen activator (tPa) to enhance secretion. New SOSIP genes were synthesized by Life Technologies with flanking PST1/NOT1 restriction sites and subsequently cloned into the pPPI4 mammalian expression vector (26). BG505.c2 and MG505.e1 SOSIP expression vectors were obtained from John Moore and colleagues. In their originally published forms, these genes contained several added sequons for N-linked glycans in a conserved binding site for the monoclonal antibody 2G12. To better mimic native antigenicity of the viral

isolate, we reverted these glycan motifs to their wildtype sequences in the BG505 and MG505 SOSIPs using site-directed mutagenesis (Agilent).

**Protein production and purification.**

SOSIPs were produced by transient transfection with either 2x PEI or Freestyle Max Reagent (Life Technologies) in suspension 293F cell at between 0.8 and 1.2 million cells/mL. Co-transfection of furin in pcDNA.3 at a ratio of three SOSIP to one furin ensured efficient proteolytic cleavage between gp120 and gp41 subunits during production. Six or seven days after transfection, supernatants were cleared by centrifugation and filtered through a 0.2 micron vacuum filtration unit and supplemented with protease inhibitors (Roche) and sodium azide to prevent microbial growth. Supernatants were incubated with *Galanthus nivalis* lectin (GNL) coupled to agarose beads overnight at 4˚C, washed with 20 mM Tris pH 7.4, 1 mM EDTA, 1 mM EGTA, 0.02% azide, 120 mM NaCl and glycoproteins eluted with 7-10 CV of 1M alpha methyl mannopyrannoside dissolved in 20 mM Tris pH 7.4, 1 mM EDTA, 1 mM EGTA, 0.02% azide, 120 mM NaCl. .

GNL eluates were concentrated using amicon ultrafiltration units (100 kDa nominal molecular weight cutoff) and buffer exchanged to DEAE low salt buffer (20 mM Tris pH 8.0, 100 mM NaCl) before loading on a 5 mL pre-packed HiTrap DEAE anion-exchange column (GE Life Sciences). Following 10 minutes of isocratic flow in 100 mM NaCL, a gradient to 1 M NaCl was initiated and fractions collected throughout. Alternatively, this step was done in batches while collecting the low salt flow through, with a final elution of bound material with 1 NaCl.

The DEAE flow through was buffer exchanged into 2 M ammonium sulfate, 0.1 M phosphate pH 7.0 and loaded onto a ProPac HIC-10 column (Dionex). A linear gradient of 2 M to 0 M ammonium sulfate in 0.1M phosphate pH 7 over 90 minutes was sufficient to resolve trimers from dimers and monomers. Lastly, the early eluting fractions (containing native-like trimer) were concentrated prior to loading on a superdex S200PG size exclusion chromatography column in PBS (20 mM sodium phosphate pH 7.4, 150 mM sodium chloride,

0.02% sodium azide). Peak fractions were collected and concentrated for downstream analyses of purity and antigenicity.

PGT145 pure BG505.c2 T332N SOSIP trimer was provided by John Moore and colleagues (original study described in (4)). BG505.c2 T332N gp120 was produced and purified in house by transient transfection of 293F cells, GNL affinity chromatography as previously described, and SEC on the superdex S200PG column.

**SDS-PAGE and BN-PAGE analyses.**

SDS denaturing and blue-native PAGE (BN-PAGE) analyses with precast gels (NOVEX) were performed to assess the oligomeric species present at each stage of our purification. The addition of 0.1 M DTT to denatured samples allowed us to ensure that furin cleavage between gp120 and gp41 subunits was complete in our SOSIPs. Typically, between 10 and 15 µg of protein was loaded per lane for BN-PAGE analysis and 5 µg per lane was loaded for SDS-PAGE analysis.

**Dynamic light Scattering.**

Dynamic light scattering measurements were performed on a Dynapro Nanostar (Wyatt Technologies). Trimer samples were diluted to 1 or 3 mg/mL in PBS and centrifuged at 15000 *x g* for 20 minutes prior to loading 8 µl into a low volume quartz cuvette. The mean estimated radius, polydispersity, and molecular weight were generated from 40 acquisitions of 5 s at 20˚C. Following these initial acquisitions, 10 µl of parafin oil was gently added to the top of the sample prior to temperature scans from 30 to 80˚C at a rate of 1˚C/min to determine the onset of SOSIP melting/aggregation.

**Negative stain-electron microscopy (NS-EM).**

A 3 µl aliquot of purified SOSIP**,** diluted to 10 or 30 µg/ml in PBS was applied for 60 s to glow discharged C-Flat, 300 mesh, Cu grids (Electron Microscopy Sciences) and stained for an additional 60 s using Nano-W (Nanoprobes). Data were collected using a FEI Tecnai T12 transmission electron microscope operating at 120 keV. Images were collected using a Gatan

4k × 4k CCD at a magnification of 52,000× at 1.0 μm defocus corresponding to a pixel size of 2.07 Å. Particles were selected using interactive particle picking in EMAN2.1 image processing suite. For each data set a phase-flipped, CTF-corrected stack containing ~20,000 particles were created and subjected to reference-free 2D classification to generate ~125 classes. Class averages containing multiple trimers within the particle box size were omitted and a representative class average for each isolate was chosen for clarity.

**Biolayer interferometry measurement of antibody-Env binding**.

Biolayer interferometry (BLI) on an Octet red platform (ForteBio) was used to assess antigenic profiles of new SOSIPs purified by our method. Our measurements were performed in an assay buffer composed of phosphate buffered saline supplemented with 1% BSA, 0.03% Tween 20, and 0.01% azide at a shake speed of 1000 rpm and 30˚C. Tip regeneration between measurements was performed in 1 M glycine at pH 2.5. In a typical binding experiment, antibodies of interest and SOSIPs were diluted in assay buffer. We diluted antibodies to 8 ug/mL for loading onto dip and read biosensors coated in anti-human IgG. We diluted SOSIP analytes to a single concentration of 125 nM to assay association. Antigenicity screens were carried out as two independent replicates unless material was limiting (PVO.4).

The area in nm·s under each association/dissociation curve was calculated using PRISM (Graphpad) and a heat map was generated based on these values to compare binding of SOSIPs to different antibodies. A smaller panel of antibodies was used for PVO.4, for which material was limiting. The area under the curve heatmap for PVO.4 binding is separated in **FIG 6** because association and dissociation times for these experiments differed from those used in the larger panel, making the inter-SOSIP comparison for this construct impossible at this time.

**Hydrogen/Deuterium-exchange mass spectrometry.**

~2ugs of protein for each time point was incubated at 22-25˚C (RT) in a buffer containing deuterium (20 mM $Na_3PO_4$ pH 7.4, 150 mM NaCl, 0.02% sodium azide, 1 mM EDTA, 85% $D_2O$). The time course extended from 3 s to 20 h and each time point was incubated in

duplicate. Samples were quenched by mixing 1:1 with 200mM TCEP, 0.02% formic acid for a final pH of 2.5 and flash frozen in liquid nitrogen. The zero time point was accomplished by pre-mixing the deuterated buffer and quench solution before addition of protein. A fully deuterated control was also included where denatured proteins (pre-treated for 15 min at 85 ˚C in 1M DTT and 3M GndHCl) were deuterated for 1hr at 85 ˚C.

LC-MS analysis was performed on a Waters Synapt G2-Si Q-TOF with a M class Aquity solvent delivery system. Samples were thawed briefly on ice and immediately injected onto a Waters HDX Manager kept at 1˚C. Samples were passed over a 2.1x50mm column filled with POROS-coupled pepsin at 150uL/min and trapped onto a BEH 2.1x5mm 1.7u C18 trap column,. Peptides were resolved over a 1x100mm BEH 1.7u C18 column (Waters) with a linear gradient of 5%B to 50% B in 10 minutes (A: 0.1% FA, 0.04% TFA 5% ACN; B: 0.1%FA 100% ACN). Source and desolvation temperatures were 70 ˚C and 130 ˚C, respectively, and the StepWave ion optics settings were adjusted to minimize loss of deuterium during ionization. Peptides were assigned from $MS^E$ measurements on undeuterated samples using PLGS (Waters) in combination with exact mass and known elution times from previous examinations of similar SOSIP constructs. Deuterium exchange kinetics were analyzed using HX-express v2. Percent exchange is reported relative to the zero and fully deuterated samples. One set of data was lost during processing resulting in only a single replicate time point for MG505 at 20 hours. An internal peptide standard was included in each sample to control for differences in ambient temperature at the time the experiments were performed (Pro-Pro-Pro-Ile or PPPI).

## RESULTS

### Diverse Envs engineered as SOSIP.v1 vary widely in abundance of different conformers.

We examined six HIV-1 Env variants primarily from acute stages of infection, including both sexually and vertically transmitted viruses (**TABLE 1**); these Envs were from clades A and B and included a well-characterized, infant-derived Env, BG505.c2 (here in its wildtype form,

lacking a glycan modification at position 332 (40), which was introduced into some SOSIP.v1 trimers to promote binding to glycan-specific Mabs like 2G12 (26)).

When the six SOSIPs were purified by lectin affinity chromatography alone (sample analytical SEC shown in **FIG 1**; analytical data for all SOSIPs shown in **FIG 2**), BN-PAGE analysis revealed that all contained some fraction of trimer-sized species, but that the relative abundance of trimers, dimers, and monomers—which, as glycoproteins, run heavier than expected on the native gel at ~700, 450 and 220 kDa, respectively—varied significantly across the panel (BN-PAGE left of NS-EM micrograph in **FIG 2**); the amount of Env material that was aggregated and did not enter the native gel also varied among isolates but proved difficult to quantify by this method.

To quantify relative amounts of each Env species present after GNL affinity, we used size exclusion chromatography (SEC). In the SEC chromatograms shown in **FIG 2**, each elution profile could be deconvolved into 3 major overlapping Gaussian peaks—corresponding to different oligomeric Env species (fits are shown in orange, blue, and red). The earliest eluting peak was composed of large aggregates eluting in the void volume of the SEC (orange trace in **FIG 2** chromatogram). This aggregated materials contributed between 9 and 34% of the total mixture depending on the specific Env. The third peak (red trace) accounted for 19-38% of the concentrated protein eluting off SEC and was composed of a heterogeneous mixture of monomeric and dimeric Env as assessed by BN-PAGE.

The middle peak in each chromatogram (blue trace in **FIG 2A** SEC chromatograms) contained the majority of NL trimer among all the fractions for each Env as assessed by non-reducing SDS-PAGE and confirmed by NS-EM. For the well-characterized BG505.c2 Env, by SEC, ~53% of the total protein eluted in this peak which had its $A_{280}$ maximum in a similar position to purified NL glycosylated SOSIP trimers (14, 35, 41), but with a broader elution profile. In general, the other Envs had smaller amounts of protein that eluted in this middle peak ranging from ~35% in PVO.4 to 49% in MG505; all except MG505 were somewhat lower and significantly broader than for BG505.c2. For BG505.c2, on a non-reducing SDS-PAGE gel, the

307 protein in this central peak was found to consist primarily of disulfide-bonded, cleaved gp120-
308 $gp41_{ecto}$ SOSIP protomers that run close to 140 kDa (**FIG 2B**). However the gel analysis also
309 revealed that the middle SEC peak contained significant, though variable, fractions of aberrantly
310 disulfide bonded dimeric contaminants (**FIG 2B**).

311 NS-EM enabled us to qualitatively assess trimeric structures present in the peak $A_{280}$-
312 absorbing fraction eluting in the central SEC peak for each Env. This peak trimer fraction was
313 observed to contain significant amounts of recognizable NL trimers along with other non-native
314 Env species (representative trimer structures boxed in green in micrographs of **FIG 2A**).
315 However, the ratio of NL trimer to non-native appearing structures varied among Envs, even in
316 this peak SEC fraction, with BG505.c2, KNH1144, and MG505.e1 producing more particles
317 consistent with NL SOSIP Envs relative to the others such as PVO.4 and BF520.e3, which
318 showed fairly low abundance of recognizable NL trimers at this stage of purification.

319
320 **DEAE weak anion-exchange removes aggregated Env.**

321 Since GNL affinity alone yielded, at best, roughly half purified NL trimer, we next tested
322 whether an additional ion exchange step would help to remove aggregates and misfolded forms
323 of Env (refer to **FIG 1** for purification scheme). In **FIG 3A** we show the DEAE anion-exchange
324 chromatogram (following GNL affinity purification) from our purification of BF520.e3 SOSIP
325 trimer, which is representative of how all the Envs behaved. SEC analysis of the resulting post-
326 ion exchange step, BN and SDS-PAGE analyses of the Env species are also shown. We
327 observed that the NL Env population flowed through the ion exchange column under low salt
328 conditions (peak 1 in **FIG 3A** that was collected during the 100 mM NaCl isocratic flow stage of
329 the chromatography run), while aggregated forms of Env and other contaminants were retained
330 by the column and only eluted in high salt (Peak 2 eluting in a gradient that increased salt
331 concentration to 1 M NaCl). The protein from each of these peaks was collected and subjected
332 to analytical SEC to identify the oligomeric species that were present in the respective peaks.
333 The DEAE flow through appeared to contain the Env species corresponding to trimer, dimer,
334 and monomer (referenced to blue and red fitted traces in **FIG 2A** SEC chromatograms). The

SEC profile for the DEAE eluate (shown in red **FIG 3A**) matched the aggregated protein eluting in the void of the SEC column as observed from the GNL affinity SEC profiles shown in **FIG 2A**. When the trimer peak fractions from the DEAE flow through (first peak in blue trace **FIG 3A**) were analyzed by BN-PAGE it was clear that this material was primarily trimeric and dimeric Env. The same analysis of the DEAE eluate showed an aggregated smear by BN-PAGE and extensive laddering by SDS-PAGE **(FIG 3A)**. We thus found that by adding a DEAE weak anion-exchange purification step after GNL affinity chromatography, we could separate NL trimer and smaller Env sub-assemblies from a more heterogeneous mixture of contaminants and aggregates produced by lectin affinity alone.

**Hydrophobic interaction chromatography separates native-like Env trimers from other species.**

Next we tested whether hydrophobic interaction chromatography (HIC) applied after the DEAE ion exchange step could further enrich NL trimer and remove contaminating dimer and monomer fractions from the mixture of Env conformers. In **FIG 3B** we show a representative HIC chromatogram from the purification of BF520.e3 SOSIP (second to last step shown in **FIG 1** purification scheme). Again, two primary populations were observed following separation by a salt gradient. The early peak (blue 1 in **FIG 3B**) eluted with baseline resolution before the second eluting peak (red 2 in **FIG 3B**), which only came off the column toward the end of the gradient. Each of these peaks was pooled and analytical SEC was run to determine the species that were present. Peak 1 from HIC (blue SEC trace **FIG 3B**), when passed over the SEC column, eluted in a narrow, symmetrical profile at the expected volume for NL trimeric Env (~54 mL). By BN-PAGE and reducing, and non-reducing SDS-PAGE, this material appeared to consist of homogenous, cleaved, NL trimeric Env (see gel panel in **FIG 3B**). When passed through the analytical SEC column, the material from peak 2 of the HIC step eluted as two overlapping peaks (red trace **FIG 3B**). By BN and reducing and non-reducing SDS-PAGE, this HIC peak 2 material appeared to contain only dimeric and monomeric Env (gel panel **FIG 3B**). Based on these analyses it became clear why GNL affinity and SEC were insufficient to purify

SOSIP trimers to homogeneity in analysis from **FIG 2A**. The dimeric species seen in the SEC trace of the second HIC peak clearly co-eluted with the entirety of the true NL trimer.

In contrast to the multiple, overlapping peaks that were observed for preparations that only were processed by lectin-affinity (**FIG 2A**), when the HIC-purified early eluting peak for all six Envs was polished by SEC, we observed a single, well-resolved peak consistent in breadth and retention time with purified trimers for all Envs tested (**FIG 4A**). These peaks eluted consistently at ~54 mL, which corresponds closely to the predicted molecular weight of SOSIP trimers (37)(26). BN-PAGE analysis also demonstrated that the purified SOSIP trimer preparations contained only the trimer populations, with little trace of possible non-native sub-assemblies. By NS-EM, the predominance of NL trimer structures in the purified material was clearly evident (**FIG 4A**). When the final material was run on reducing and non-reducing SDS-PAGE (representative data from BF520.e3 SOSIP in **FIG 3B** gel panel), it was also clear that all of the Env present was in properly cleaved gp120-gp41 form as DTT reducing agent reverted the SOSIP disulfide-bonded gp120-gp41 to individual gp120 and gp41 subunits. These data confirmed that our method successfully separated cleaved, NL trimer from all other components of the mixture of Env assemblies produced by transient transfection in 293F cells.

Yields of NL trimer varied among isolates with BG505.c2, MG505.e1, and KNH1144 producing 1-2 mg of NL trimer per liter of transfection, which was higher than for other Envs. We found that PVO.4 produced as little as 0.1 mg/L, necessitating significant scale up to generate sufficient protein for our studies and even then limiting the antigenicity experiments we could undertake for this study. Nevertheless, even in this case where the fraction of NL trimer was minor, the data show that the desirable sub-population could be isolated and purified to homogeneity.

**Dynamic light scattering confirms that the purified trimer material is monodisperse and of the expected size.**

Dynamic light scattering (DLS) was used to measure the polydispersity of purified trimer preparations and the hydrodynamic radii of our HIC-purified SOSIP trimers in solution. This

method can detect small levels of aggregation and contamination that may be difficult to assess by other methods such as BN-PAGE or SEC. All preparations showed a polydispersity of less than 7% indicating that the samples were highly monodisperse and not significantly contaminated with other oligomeric species. Hydrodynamic radii measured by DLS ranged between 6.6 and 6.9 nm—consistent with trimer dimensions observed by NS-EM (**Table 2**).

DLS was also used to measure the thermal stability of the various SOSIP trimers. In this case, DLS measurements were gathered as the temperature of the thermostated sample cuvette was gradually increased from 20 to 80 ˚C. All trimers exhibited a stable baseline and single transition onset between 60 and 70 ˚C—consistent with the thermal stability seen in previous studies of SOSIP trimers (26, 37, 38) (representative melting curves shown in **FIG 4B**). Following the temperature-induced transition, the majority of the samples adopted some larger form of trimer that subsequently appeared to aggregate, as indicated by the dramatic increase in apparent particle dimensions above ~80 ˚C (data not shown). The BS208 SOSIP.v1 trimer, showed a different phenotype in that it did not exhibit a clear onset of melting or transition prior to aggregation at extremely high temperatures (~85 ˚C) (purple trace in **FIG 4B**).

**HDX-MS to probe local structural order and conformational state**

We used HDX-MS to examine whether the HIC-purified SOSIP trimers exhibited exchange profiles and local structural organization consistent with NL trimers. The deuterium uptake profiles for peptides covering N/C gp120 termini, V2, V3 and gp41 segments, which are diagnostic of NL trimer formation (uptake profiles shown in **FIG 5**) (14, 17), were in excellent agreement with previously reported data from our group for PGT145-purified BG505.c2 (T332N mutant) (4). Only subtle differences between PGT145 pure and HIC-purified material were apparent, which likely originate from the two data sets having been collected at different times with slightly different ambient conditions, an effect that is apparent in the PPPI internal standard, a recombinant tetra-peptide included to probe for such differences (**FIG 5**). In contrast, HDX-MS data for monomeric gp120 from BG505.c2 T332N showed a considerably less ordered profile based upon these diagnostic peptides. The monomeric gp120 behaved in a manner consistent

with the V1/V2 and V3 lacking stabilizing interactions, and the N/C termini likewise were highly dynamic in the absence of interactions with a gp41 subunit. Among the trimers, some individual segments did show isolate-specific differences such as in the case of BF520.e3, which appears to present a more dynamic V2 loop relative to the other SOSIP trimers. The rest of the diagnostic peptides for BF520.e3 are in excellent agreement with the other trimers and indicate that the differences are primarily localized to the V1/V2 apex.

**Monoclonal antibody recognition of HIC-purified SOSIP trimers**

Using biolayer interferometry to measure binding of the purified trimers to IgG captured on the Octet sensors, we observed diverse antigenic profiles for our HIC-pure SOSIP trimers against a panel of HIV specific Mabs with known epitopes **(FIG 6)**. BG505.c2, MG05.e1, PVO.4 and KNH1144 bound robustly (areas under single binding curves ranging from 153 to 170 nm·s) to V1/V2 quaternary specific antibody PGT145. Binding was lower (7 to 19 nm·s) for BS208.b1—an Env with notably short loops at its apex—and for KNH1144 (T162A), a mutant we purified by the same method lacking a critical glycan for PGT145 binding. BF520.e3 bound PGT145 with strong and rapid association and relatively fast dissociation, likely resulting in weak affinity.

HIC-purified SOSIP trimers also showed low binding (<40 nm·s) over short periods to F105, b12, and 17b—antibodies with epitopes that are difficult to access and bind in the NL trimeric conformation (10) of most Env isolates studied to date. Notable exceptions included KNH1144 and BS208.b1, which both bound to b12 and to some extent to F105. As a negative control for Octet BLI-monitored antibody binding we included 2F5, an MPER antibody, targeting an epitope not present in SOSIP trimers. None of the HIC-purified trimers showed appreciable binding to this negative control IgG.

It is important to note that timings were consistent across this panel for association and dissociation for all variants except PVO.4, for which limited material prevented a repeat experiment with identical timing to the other curves. For this reason, we have offset the PVO.4

446 binding data in **FIG 6** and compared curves internally to only other PVO.4:Ab interactions. We
447 also note that a single concentration was not sufficient to rigorously derive kinetic parameters
448 for these interactions. While we can conclude semi-quantitatively that certain interactions are
449 high-binding or low-binding and attribute these observations to either rapid or slow association
450 and dissociation phases, we cannot definitively compare similar interactions using this screen.

451
452 **DISCUSSION**

453 We present a scalable approach for purifying native-like (NL) SOSIP trimers that does
454 not require HIV-specific monoclonal antibodies. The combination of lectin affinity, anion-
455 exchange, hydrophobic interaction chromatography, and SEC was sufficient to separate NL
456 trimer from non-native conformations in preparations of SOSIPs engineered from multiple
457 diverse Envs, many derived from acute and T/F viruses. Based on the level of purity obtained
458 for these Env SOSIPs, we propose that this approach could be used in the place of or perhaps
459 in addition to existing affinity methods for the purification of NL trimeric immunogens, which
460 have become promising candidates for HIV-1 vaccines. And because other modified forms of
461 engineered, soluble trimer such as “NFL” or “NFL TD” (42) and “single-chain” (43) are likely to
462 display similar biochemical profiles with the hydrophilic glycan shield presented on the exterior
463 of natively structured assemblies, we anticipate that the purification approach we describe will
464 also be effective in isolating the NL trimeric population from these recombinant systems.

465 In addition to applications in immunogen production, our method enables study of variant
466 specific Env structural features, which may underlie differences in antigenicity and function. Our
467 initial structural analysis by HDX-MS and NS-EM of this panel of Env SOSIP trimers
468 demonstrated that, while our purified trimers retain the closed, pre-fusion NL Env conformation,
469 some specific structural differences were identifiable, and some of these appear to correlate
470 with antigenic differences. By HDX-MS, the BF520.e3 trimer shared similar structural order in
471 regions probed by most diagnostic peptides, however in peptides from V2, spanning 165-181,
472 significant deuterium exchange was observed, suggesting that those stretches of V2 may be
473 more dynamic and exposed in this trimer than in other Envs (**FIG 5**). This property was

474 accompanied by a distinct mode of interaction with the quaternary-specific BNAb PGT145, an
475 antibody that does not neutralize the corresponding BF520.e3 pseudovirus, but does bind
476 strongly to transiently expressed Env on the surface of cells. The epitope for PGT145 is located
477 proximal to the V2 segment where deuterium uptake was rapid in this BF520.e3 trimer and we
478 observed rapid association—comparable to those observed for BG505.c2 and MG505.e1. The
479 dissociation, however, was considerably faster, suggesting a highly specific, but transient
480 interaction was taking place, which may be attributable to a difference in Env structural
481 dynamics in the transition of this isolate from “closed” to “open” prefusion conformations.

482 Characterization of trimer organization by NS-EM also revealed apparent structural
483 differences of one Env variant, BS208.b1—which displayed trimeric lobes that were more
484 slender and lacked the curved, blade-like propeller morphology seen in the other trimers (**FIG**
485 **4A**). We hypothesize that this difference could be related to the differences in V1/V2 interactions
486 at the apex of the BS208.b1 trimer relative to Envs such as BG505.c2 (**Table 1**). BS208.b1 has
487 relatively short V1/V2 loops, with fewer potential N-linked glycosylation sites, compared to the
488 other trimers we examined, for example V1 length in BS208.b1 is 13 vs 17 in BG505.c2, and V2
489 lengths are 42 vs 46. As in the case of the BF520.e3 SOSIP, BS208.b1 trimers interact weakly
490 with the antibody PGT145, suggesting that a change in organization and presentation of the
491 antibody’s epitope at the apex exists in BS208.b1 trimers, despite conservation of the N160 and
492 N156 glycosylation sites that are often targeted by this class of antibodies (**FIG 6**). The distinct
493 morphology and variable loop organization may also relate to the robustness of this Env to
494 thermal perturbation, where the DLS-monitored thermal melts indicated that BS208.b1 trimers
495 show a delayed onset of melting and aggregation (**FIG 4B)**.

496 Because BF520.e3, BS208.b1, and KNH1144 T162A SOSIPs have structural features
497 that ablate or perturb high affinity interactions with the quaternary specific antibody PGT145, we
498 propose that these and similar Envs would be poor candidates for purification by current
499 PGT145-based procedures (37). In such cases, we would predict very low yields due to low
500 affinity or negligible binding of these Envs to the PGT145 affinity column. We further propose

that inability to purify by PGT145 is not necessarily globally diagnostic of poor or deficient trimer formation. Clearly, native and functional envelope trimer is produced for these variants given that the corresponding pseudotyped viruses are infectious (40, 44). Our results suggest that the SOSIP-modified, soluble forms of these Env variants retain NL trimeric structure. Our approach thus appears to have significant and broad utility in isolating NL trimers from antigenically and phenotypically diverse Envs, including those that would be challenging to purify using PGT145-affinity approaches.

In summary, we have developed a new method for NL Env trimer purification that separates Env conformers based upon their general biochemical/biophysical properties such as surface charge and exposure of hydrophobic patches. This procedure produces highly pure NL Env and avoids the need for using Env-specific Mabs. With this method, we have demonstrated the application to diverse Env trimers that retain unique structural properties such as localized structural differences that are detectable by HDX-MS. These structural differences in specific regions within the context of overall NL trimers, showed reasonable correlations with antibody binding to those specific sites and epitopes. With the ability to isolate diverse NL Env trimers, we anticipate that it will be possible to expand our understanding of structural, phenotypic variation in HIV-1 as well as to provide reagents for immunogen production.

**ACKNOWLEDGEMENTS**

This work was supported by NIH grants R21-AI112389 (KKL), R01-AI120961 (JO), and through the Bill and Melinda Gates Foundation Collaboration for AIDS Vaccine Discovery (CAVD) grant OPP1033102 (SLH) and the Global Health Vaccine Accelerator Program grant OPP1126258 (KKL). We would like to thank John Moore and colleagues for providing the BG505.c2 T332N and un-mutated MG505.e1 SOSIP constructs, which were reverted for this study. The following reagents were obtained through the NIH AIDS Research and Reference Reagent Program: CD4-IgG2 was from Progenics Pharmaceuticals, Inc.; HIV-1 gp120 monoclonal antibodies 17b from James E. Robinson; VRC01 from John Mascola; F105 from Marshall Posner and Lisa

528 Cavacini; b12 from Dennis Burton and Carlos Barbas; 3074 from Susan Zolla-Pazner; 2G12
529 and 2F5 from Herman Katinger; and PGT121, PGT126 and PGT145 from IAVI.
530
531

532 **REFERENCES**


533 1. Gao F, Weaver EA, Lu Z, Li Y, Liao H-X, Ma B, Alam SM, Scearce RM, Sutherland LL, Yu
534 J-S, Decker JM, Shaw GM, Montefiori DC, Korber BT, Hahn BH, Haynes BF. 2005.
535 Antigenicity and Immunogenicity of a Synthetic Human Immunodeficiency Virus Type 1
536 Group M Consensus Envelope Glycoprotein. J Virol 79:1154–1163.

537 2. Beddows S, Schülke N, Kirschner M, Barnes K, Franti M, Michael E, Ketas T, Sanders
538 RW, Maddon PJ, Olson WC, Moore JP. 2005. Evaluating the Immunogenicity of a
539 Disulfide-Stabilized, Cleaved, Trimeric Form of the Envelope Glycoprotein Complex of
540 Human Immunodeficiency Virus Type 1. J Virol 79:8812–8827.

541 3. Cheng C, Pancera M, Bossert A, Schmidt SD, Chen RE, Chen X, Druz A, Narpala S,
542 Doria-Rose NA, McDermott AB, Kwong PD, Mascola JR. 2016. Immunogenicity of a
543 Prefusion HIV-1 Envelope Trimer in Complex with a Quaternary-Structure-Specific
544 Antibody. J Virol 90:2740–2755.

545 4. De Taeye SW, Ozorowski G, Torrents de la Peña A, Guttman M, Julien J-P, van
546 den Kerkhof TLGM, Burger JA, Pritchard LK, Pugach P, Yasmeen A, Crampton J, Hu J,
547 Bontjer I, Torres JL, Arendt H, DeStefano J, Koff WC, Schuitemaker H, Eggink D, Berkhout
548 B, Dean H, LaBranche C, Crotty S, Crispin M, Montefiori DC, Klasse PJ, Lee KK, Moore
549 JP, Wilson IA, Ward AB, Sanders RW. 2015. Immunogenicity of Stabilized HIV-1 Envelope
550 Trimers with Reduced Exposure of Non-neutralizing Epitopes. Cell 163:1702–1715.

551 5. Yang X, Wyatt R, Sodroski J. 2001. Improved Elicitation of Neutralizing Antibodies against
552 Primary Human Immunodeficiency Viruses by Soluble Stabilized Envelope Glycoprotein
553 Trimers. J Virol 75:1165–1171.

554 6. Sliepen K, Ozorowski G, Burger JA, van Montfort T, Stunnenberg M, LaBranche C,
555 Montefiori DC, Moore JP, Ward AB, Sanders RW. 2015. Presenting native-like HIV-1
556 envelope trimers on ferritin nanoparticles improves their immunogenicity. Retrovirology 12.

557 7. Tran K, Poulsen C, Guenaga J, Val N de, Wilson R, Sundling C, Li Y, Stanfield RL, Wilson
558 IA, Ward AB, Hedestam GBK, Wyatt RT. 2014. Vaccine-elicited primate antibodies use a
559 distinct approach to the HIV-1 primary receptor binding site informing vaccine redesign.
560 Proc Natl Acad Sci 111:E738–E747.

561 8. Chen L, Kwon YD, Zhou T, Wu X, O'Dell S, Cavacini L, Hessell AJ, Pancera M, Tang M,
562 Xu L, Yang Z-Y, Zhang M-Y, Arthos J, Burton DR, Dimitrov DS, Nabel GJ, Posner MR,
563 Sodroski J, Wyatt R, Mascola JR, Kwong PD. 2009. Structural Basis of Immune Evasion at
564 the Site of CD4 Attachment on HIV-1 gp120. Science 326:1123–1127.

565 9. Stewart-Jones GBE, Soto C, Lemmin T, Chuang G-Y, Druz A, Kong R, Thomas PV, Wagh
566 K, Zhou T, Behrens A-J, Bylund T, Choi CW, Davison JR, Georgiev IS, Joyce MG, Kwon
567 YD, Pancera M, Taft J, Yang Y, Zhang B, Shivatare SS, Shivatare VS, Lee C-CD, Wu C-Y,
568 Bewley CA, Burton DR, Koff WC, Connors M, Crispin M, Baxa U, Korber BT, Wong C-H,
569 Mascola JR, Kwong PD. 2016. Trimeric HIV-1-Env Structures Define Glycan Shields from
570 Clades A, B, and G. Cell 165:813–826.

571 10. Wei X, Decker JM, Wang S, Hui H, Kappes JC, Wu X, Salazar-Gonzalez JF, Salazar MG,
572 Kilby JM, Saag MS, Komarova NL, Nowak MA, Hahn BH, Kwong PD, Shaw GM. 2003.
573 Antibody neutralization and escape by HIV-1. Nature 422:307–312.

574 11. Derking R, Ozorowski G, Sliepen K, Yasmeen A, Cupo A, Torres JL, Julien J-P, Lee JH,
575 Montfort T van, Taeye SW de, Connors M, Burton DR, Wilson IA, Klasse P-J, Ward AB,
576 Moore JP, Sanders RW. 2015. Comprehensive Antigenic Map of a Cleaved Soluble HIV-1
577 Envelope Trimer. PLOS Pathog 11:e1004767.

578 12. Eckert DM, Kim PS. 2001. Mechanisms of viral membrane fusion and its inhibition. Annu
579 Rev Biochem 70:777–810.

580 13. Park HE, Gruenke JA, White JM. 2003. Leash in the groove mechanism of membrane
581 fusion. Nat Struct Mol Biol 10:1048–1053.

582 14. Guttman M, Garcia NK, Cupo A, Matsui T, Julien J-P, Sanders RW, Wilson IA, Moore JP,
583 Lee KK. 2014. CD4-Induced Activation in a Soluble HIV-1 Env Trimer. Structure 22:974–
584 984.

585 15. Sattentau QJ. 2013. Envelope Glycoprotein Trimers as HIV-1 Vaccine Immunogens.
586 Vaccines 1:497–512.

587 16. Ringe RP, Sanders RW, Yasmeen A, Kim HJ, Lee JH, Cupo A, Korzun J, Derking R,
588 Montfort T van, Julien J-P, Wilson IA, Klasse PJ, Ward AB, Moore JP. 2013. Cleavage
589 strongly influences whether soluble HIV-1 envelope glycoprotein trimers adopt a native-like
590 conformation. Proc Natl Acad Sci 110:18256–18261.

591 17. Guttman M, Lee KK. 2013. A Functional Interaction between gp41 and gp120 Is Observed
592 for Monomeric but Not Oligomeric, Uncleaved HIV-1 Env gp140. J Virol 87:11462–11475.

593 18. Yasmeen A, Ringe R, Derking R, Cupo A, Julien J-P, Burton DR, Ward AB, Wilson IA,
594 Sanders RW, Moore JP, Klasse PJ. 2014. Differential binding of neutralizing and non-
595 neutralizing antibodies to native-like soluble HIV-1 Env trimers, uncleaved Env proteins,
596 and monomeric subunits. Retrovirology 11:41.

597 19. Guttman M, Cupo A, Julien J-P, Sanders RW, Wilson IA, Moore JP, Lee KK. 2015.
598 Antibody potency relates to the ability to recognize the closed, pre-fusion form of HIV Env.
599 Nat Commun 6:6144.

600 20. Gorman J, Soto C, Yang MM, Davenport TM, Guttman M, Bailer RT, Chambers M,
601 Chuang G-Y, DeKosky BJ, Doria-Rose NA, Druz A, Ernandes MJ, Georgiev IS, Jarosinski
602 MC, Joyce MG, Lemmin TM, Leung S, Louder MK, McDaniel JR, Narpala S, Pancera M,
603 Stuckey J, Wu X, Yang Y, Zhang B, Zhou T, Program NCS, Mullikin JC, Baxa U, Georgiou

604 G, McDermott AB, Bonsignori M, Haynes BF, Moore PL, Morris L, Lee KK, Shapiro L,
605 Mascola JR, Kwong PD. 2016. Structures of HIV-1 Env V1V2 with broadly neutralizing
606 antibodies reveal commonalities that enable vaccine design. Nat Struct Mol Biol 23:81–90.

607 21. Julien J-P, Lee JH, Cupo A, Murin CD, Derking R, Hoffenberg S, Caulfield MJ, King CR,
608 Marozsan AJ, Klasse PJ, Sanders RW, Moore JP, Wilson IA, Ward AB. 2013. Asymmetric
609 recognition of the HIV-1 trimer by broadly neutralizing antibody PG9. Proc Natl Acad Sci
610 110:4351–4356.

611 22. Sanders RW, Vesanen M, Schuelke N, Master A, Schiffner L, Kalyanaraman R, Paluch M,
612 Berkhout B, Maddon PJ, Olson WC, Lu M, Moore JP. 2002. Stabilization of the Soluble,
613 Cleaved, Trimeric Form of the Envelope Glycoprotein Complex of Human
614 Immunodeficiency Virus Type 1. J Virol 76:8875–8889.

615 23. Schülke N, Vesanen MS, Sanders RW, Zhu P, Lu M, Anselma DJ, Villa AR, Parren PWHI,
616 Binley JM, Roux KH, Maddon PJ, Moore JP, Olson WC. 2002. Oligomeric and
617 Conformational Properties of a Proteolytically Mature, Disulfide-Stabilized Human
618 Immunodeficiency Virus Type 1 gp140 Envelope Glycoprotein. J Virol 76:7760–7776.

619 24. Binley JM, Sanders RW, Master A, Cayanan CS, Wiley CL, Schiffner L, Travis B,
620 Kuhmann S, Burton DR, Hu S-L, Olson WC, Moore JP. 2002. Enhancing the proteolytic
621 maturation of human immunodeficiency virus type 1 envelope glycoproteins. J Virol
622 76:2606–2616.

623 25. Sanders RW, Schiffner L, Master A, Kajumo F, Guo Y, Dragic T, Moore JP, Binley JM.
624 2000. Variable-Loop-Deleted Variants of the Human Immunodeficiency Virus Type 1
625 Envelope Glycoprotein Can Be Stabilized by an Intermolecular Disulfide Bond between the
626 gp120 and gp41 Subunits. J Virol 74:5091–5100.

627 26. Sanders RW, Derking R, Cupo A, Julien J-P, Yasmeen A, Val N de, Kim HJ, Blattner C,
628 Peña AT de la, Korzun J, Golabek M, Reyes K de los, Ketas TJ, Gils MJ van, King CR,
629 Wilson IA, Ward AB, Klasse PJ, Moore JP. 2013. A Next-Generation Cleaved, Soluble
630 HIV-1 Env Trimer, BG505 SOSIP.664 gp140, Expresses Multiple Epitopes for Broadly
631 Neutralizing but Not Non-Neutralizing Antibodies. PLOS Pathog 9:e1003618.

632 27. Lyumkis D, Julien J-P, Val N de, Cupo A, Potter CS, Klasse P-J, Burton DR, Sanders RW,
633 Moore JP, Carragher B, Wilson IA, Ward AB. 2013. Cryo-EM Structure of a Fully
634 Glycosylated Soluble Cleaved HIV-1 Envelope Trimer. Science 342:1484–1490.

635 28. Julien J-P, Cupo A, Sok D, Stanfield RL, Lyumkis D, Deller MC, Klasse P-J, Burton DR,
636 Sanders RW, Moore JP, Ward AB, Wilson IA. 2013. Crystal Structure of a Soluble Cleaved
637 HIV-1 Envelope Trimer. Science 342:1477–1483.

638 29. Pancera M, Zhou T, Druz A, Georgiev IS, Soto C, Gorman J, Huang J, Acharya P, Chuang
639 G-Y, Ofek G, Stewart-Jones GBE, Stuckey J, Bailer RT, Joyce MG, Louder MK, Tumba N,
640 Yang Y, Zhang B, Cohen MS, Haynes BF, Mascola JR, Morris L, Munro JB, Blanchard SC,
641 Mothes W, Connors M, Kwong PD. 2014. Structure and immune recognition of trimeric
642 pre-fusion HIV-1 Env. Nature 514:455–461.

643 30. Lee JH, Ozorowski G, Ward AB. 2016. Cryo-EM structure of a native, fully glycosylated,
644 cleaved HIV-1 envelope trimer. Science 351:1043–1048.

645 31. Kwon YD, Pancera M, Acharya P, Georgiev IS, Crooks ET, Gorman J, Joyce MG, Guttman
646 M, Ma X, Narpala S, Soto C, Terry DS, Yang Y, Zhou T, Ahlsen G, Bailer RT, Chambers
647 M, Chuang G-Y, Doria-Rose NA, Druz A, Hallen MA, Harned A, Kirys T, Louder MK, O'Dell
648 S, Ofek G, Osawa K, Prabhakaran M, Sastry M, Stewart-Jones GBE, Stuckey J, Thomas
649 PV, Tittley T, Williams C, Zhang B, Zhao H, Zhou Z, Donald BR, Lee LK, Zolla-Pazner S,
650 Baxa U, Schön A, Freire E, Shapiro L, Lee KK, Arthos J, Munro JB, Blanchard SC, Mothes
651 W, Binley JM, McDermott AB, Mascola JR, Kwong PD. 2015. Crystal structure,

652 conformational fixation and entry-related interactions of mature ligand-free HIV-1 Env. Nat
653 Struct Mol Biol 22:522–531.

654 32. Harris A, Borgnia MJ, Shi D, Bartesaghi A, He H, Pejchal R, Kang Y (Kenneth), Depetris R,
655 Marozsan AJ, Sanders RW, Klasse PJ, Milne JLS, Wilson IA, Olson WC, Moore JP,
656 Subramaniam S. 2011. Trimeric HIV-1 glycoprotein gp140 immunogens and native HIV-1
657 envelope glycoproteins display the same closed and open quaternary molecular
658 architectures. Proc Natl Acad Sci 108:11440–11445.

659 33. Liu J, Bartesaghi A, Borgnia MJ, Sapiro G, Subramaniam S. 2008. Molecular architecture
660 of native HIV-1 gp120 trimers. Nature 455:109–113.

661 34. Pancera M, Zhou T, Druz A, Georgiev IS, Soto C, Gorman J, Huang J, Acharya P, Chuang
662 G-Y, Ofek G, Stewart-Jones GBE, Stuckey J, Bailer RT, Joyce MG, Louder MK, Tumba N,
663 Yang Y, Zhang B, Cohen MS, Haynes BF, Mascola JR, Morris L, Munro JB, Blanchard SC,
664 Mothes W, Connors M, Kwong PD. 2014. Structure and immune recognition of trimeric
665 prefusion HIV-1 Env. Nature 514:455–461.

666 35. Sanders RW, Derking R, Cupo A, Julien J-P, Yasmeen A, de Val N, Kim HJ, Blattner C, de
667 la Peña AT, Korzun J, Golabek M, de los Reyes K, Ketas TJ, van Gils MJ, King CR, Wilson
668 IA, Ward AB, Klasse PJ, Moore JP. 2013. A Next-Generation Cleaved, Soluble HIV-1 Env
669 Trimer, BG505 SOSIP.664 gp140, Expresses Multiple Epitopes for Broadly Neutralizing
670 but Not Non-Neutralizing Antibodies. PLoS Pathog 9.

671 36. Sanders RW, van Gils MJ, Derking R, Sok D, Ketas TJ, Burger JA, Ozorowski G, Cupo A,
672 Simonich C, Goo L, Arendt H, Kim HJ, Lee JH, Pugach P, Williams M, Debnath G, Moldt
673 B, van Breemen MJ, Isik G, Medina-Ramírez M, Back JW, Koff W, Julien J-P, Rakasz EG,
674 Seaman MS, Guttman M, Lee KK, Klasse PJ, LaBranche C, Schief WR, Wilson IA,
675 Overbaugh J, Burton DR, Ward AB, Montefiori DC, Dean H, Moore JP. 2015. HIV
676 Neutralizing Antibodies Induced by Native-like Envelope Trimers. Science 349:aac4223.

677 37. Pugach P, Ozorowski G, Cupo A, Ringe R, Yasmeen A, Val N de, Derking R, Kim HJ,
678 Korzun J, Golabek M, Reyes K de los, Ketas TJ, Julien J-P, Burton DR, Wilson IA,
679 Sanders RW, Klasse PJ, Ward AB, Moore JP. 2015. A Native-Like SOSIP.664 Trimer
680 Based on an HIV-1 Subtype B env Gene. J Virol 89:3380–3395.

681 38. Julien J-P, Lee JH, Ozorowski G, Hua Y, Peña AT de la, Taeye SW de, Nieusma T, Cupo
682 A, Yasmeen A, Golabek M, Pugach P, Klasse PJ, Moore JP, Sanders RW, Ward AB,
683 Wilson IA. 2015. Design and structure of two HIV-1 clade C SOSIP.664 trimers that
684 increase the arsenal of native-like Env immunogens. Proc Natl Acad Sci 112:11947–
685 11952.

686 39. Guenaga J, Val N de, Tran K, Feng Y, Satchwell K, Ward AB, Wyatt RT. 2015. Well-
687 Ordered Trimeric HIV-1 Subtype B and C Soluble Spike Mimetics Generated by Negative
688 Selection Display Native-like Properties. PLOS Pathog 11:e1004570.

689 40. Wu X, Parast AB, Richardson BA, Nduati R, John-Stewart G, Mbori-Ngacha D, Rainwater
690 SMJ, Overbaugh J. 2006. Neutralization escape variants of human immunodeficiency virus
691 type 1 are transmitted from mother to infant. J Virol 80:835–844.

692 41. Pugach P, Ozorowski G, Cupo A, Ringe R, Yasmeen A, Val N de, Derking R, Kim HJ,
693 Korzun J, Golabek M, Reyes K de los, Ketas TJ, Julien J-P, Burton DR, Wilson IA,
694 Sanders RW, Klasse PJ, Ward AB, Moore JP. 2015. A Native-Like SOSIP.664 Trimer
695 Based on an HIV-1 Subtype B env Gene. J Virol 89:3380–3395.

696 42. Guenaga J, Dubrovskaya V, Val N de, Sharma SK, Carrette B, Ward AB, Wyatt RT. 2016.
697 Structure-Guided Redesign Increases the Propensity of HIV Env To Generate Highly
698 Stable Soluble Trimers. J Virol 90:2806–2817.

699 43. Georgiev IS, Joyce MG, Yang Y, Sastry M, Zhang B, Baxa U, Chen RE, Druz A, Lees CR,
700 Narpala S, Schön A, Galen JV, Chuang G-Y, Gorman J, Harned A, Pancera M, Stewart-

Jones GBE, Cheng C, Freire E, McDermott AB, Mascola JR, Kwong PD. 2015. Single-Chain Soluble BG505.SOSIP gp140 Trimers as Structural and Antigenic Mimics of Mature Closed HIV-1 Env. J Virol 89:5318–5329.

44. Simonich CA, Williams KL, Verkerke HP, Williams JA, Nduati R, Lee KK, Overbaugh J. 2016. HIV-1 Neutralizing Antibodies with Limited Hypermutation from an Infant. Cell 166:77-87.

45. Sok D, Doores KJ, Briney B, Le KM, Saye-Francisco KL, Ramos A, Kulp DW, Julien J-P, Menis S, Wickramasinghe L, Seaman MS, Schief WR, Wilson IA, Poignard P, Burton DR. 2014. Promiscuous Glycan Site Recognition by Antibodies to the High- Mannose Patch of gp120 Broadens Neutralization of HIV. Sci Transl Med 6:236ra63.

713 **FIGURE LEGENDS**

714 **Figure 1. Workflow for purification of SOSIP.v1 trimers.** Stages of our preparative workflow
715 (GNL➔IEX➔HIC➔SEC) are shown with simulated chromatograms to the right of each
716 purification step. The figures in which analyses of each step are described are indicated.
717
718 **Figure 2. (A) Characterization of trimer content after GNL affinity chromatography**. We
719 summarize our initial analysis of trimer content for each Env variant. To the left of each NS-EM
720 micrograph, we show BN-PAGE analyses of eluted and concentrated protein after GNL affinity
721 with kDa molecular weight markers indicated for each. These proteins were also analyzed by
722 SEC, and analytical SEC chromatograms for proteins purified by GNL affinity are plotted with
723 elution volumes of each peak maximum indicated on the bottom x-axis (black SEC trace). Each
724 GNL profile was deconvoluted into three major peaks using Gaussian fits (orange, blue, and
725 red), and the estimated percent that each peak contributes to the overall mixture is indicated in
726 the corresponding color above the traces. The peak fraction of the central, NL trimer-containing
727 peak for each variant was further analyzed by NS-EM. Representative particles that appear
728 structurally consistent with NL trimer are boxed in each micrograph in green. **(B) SEC and non-**
729 **reducing SDS-PAGE analysis of GNL purified BG505.c2 SOSIP trimer.** The SEC
730 chromatogram profile for BG505.c2 GNL eluate is shown. Non-reducing SDS-PAGE was
731 performed on fractions from 52.5 to 57.5 mL eluting in the central trimer peak to determine if any
732 fraction was free from dimeric contaminants. gp120-gp41$_{ecto}$ SOSIP protomers, which run as
733 gp140 after heating for SDS-PAGE, are labeled as well as the dimeric contaminating material
734 which runs higher on the gel.
735
736 **Figure 3. Analyses of DEAE anion-exchange followed by hydrophobic interaction**
737 **chromatography (HIC) of GNL affinity purified ENVs (A)** A representative DEAE anion-
738 exchange chromatogram from the purification of BF520.e3 is shown with the increasing salt
739 gradient indicated in red on the right axis. A fraction from each separated component (1 and 2)

in this chromatogram was subjected to SEC chromatography for analysis. Overlaid chromatograms from this analysis are shown with the SEC profile of peak 1 indicated in blue (low salt flow-through) and the SEC profile of peak 2 (high salt eluate) indicated in red. Pooled fractions from these SEC chromatograms were further analyzed by reducing (+DTT) and non-reducing (-DTT) SDS-PAGE as well as BN-PAGE, shown in the gel panel to the right. **(B)** Trimer containing material from peak 1 (blue) off the DEAE anion-exchange was next subjected to HIC. A representative chromatogram from the purification of BF520.e3 is shown, with the decreasing salt gradient indicated on the right y-axis in red. Each separated component (peaks 1 and 2) was analyzed by SEC as in **(3a)** and the overlaid chromatograms are shown. Fractions from these SEC chromatograms were further analyzed by SDS-PAGE and BN-PAGE and these data are shown with numbers corresponding to each SEC chromatogram analyzed in the gel panel to the right.

**Figure 4. (A) Characterization of purified SOSIP trimers**. SEC chromatograms from six HIC-purified trimers are shown with peak fraction retention times indicated on the x-axis. BN-PAGE analysis of the final trimer material is shown alongside these chromatograms and an estimation of approximate yield in milligrams per liter of 293F transfection is indicated above. NS-EM micrographs and trimeric class averages of this final material for each Env are also shown. **(B) Dynamic light scattering (DLS) temperature scans of HIC-pure SOSIP trimers.** Melting temperatures were assessed by measuring the change in particle radius over the course of a temperature scan from 30˚C to 80˚C (up to 90˚C for BS208.b1). Melting was defined as a stable transition to between 9 and 15 nm from the closed-prefusion radius at baseline of ~6.8 nm. Aggregation accompanied a more dramatic transition to 100-1000 nm particle radii with multimodal polydispersity distributions (seen in the case of BS208.b1 at high temperatures).

**Figure 5. HDX-MS of HIC pure trimers.** We examined a subset of our HIC-pure SOSIP trimers using Hydrogen/Deuterium-exchange mass spectrometry (HDX-MS). Deuterium-uptake profiles

(BG505.c2 in blue, MG505.e1 in red, PVO.4 in brown, and BF520.e3 in green) are shown for N-terminal peptides of the gp120 inner domain, pre-bridging sheet segment (pre-BS), V2, V3, C-terminus, fusion peptide proximal region (FPPR) and first heptad repeat (HR1) domains. The deuterated fraction is plotted for each Env and time point in duplicate (except for MG505.e1 at the 20hr time point, for which only one data set was available). For reference, we also included data for peptides from monomeric gp120 (pink dashed line) and PGT145 purified BG505 T332N trimer (grey dashed line). Each reference data set (monomer and trimer) was collected in experiments separately from the HIC-pure trimers, under slightly different conditions and only single time points are included to establish patterns for native-like (SOSIP) and non-native (gp120) Env.

**Figure 6. Antigenicity of HIC pure trimers by biolayer interferometry.** Biolayer interferometry (BLI) analysis was used with a panel of HIV-1 specific neutralizing and non-neutralizing antibodies to assess antigenicity of trimers. For each antibody:Env interaction we show a representative binding curve (association and dissociation phases) at 125 nM SOSIP. In the section to the left of the figure, SOSIPs for which enough material was available to assess binding to the entire panel are shown (BF520.e3, BG505.c2, MG505.e1, KNH1144 +/- N160, and BS208.b1). A heat map based on area under each binding curve (nm·s), in which dark green indicates strong binding (>150 nm·s), yellow intermediate (<120 nm·s), and orange to red low or no binding (80 to 2 nm·s) on a continuous scale, is also shown for this panel to better compare these interactions. Note, BG505.c2, which lacks the N332 glycan is still bound by bNAbs that target this epitope, likely due to promiscuous glycan recognition by PGT121 and PGT126 (45). For PVO.4, in the section to the right, material was limited and the association/dissociation times used for this earlier preparation were not consistent with antigenicity data from the other SOSIPs. We therefore summarize data from this Env separately and qualitatively with green + and red x indicating strong or low to no binding respectively.

**Table 1. Summary of Env origins and traits.**

| Isolate | Origin | Transmission | Clade | Co-receptor | Infection | Tier | V1/V2 length | Predicted N-linked glycans per protomer[e] | GenBank Protein ID | Reference (PMID) |
|---|---|---|---|---|---|---|---|---|---|---|
| **BG505.c2** | NBT[a] | MTCT[b] | A | R5 | Acute | 2 | 17/46 | 24 | ABA61516.1 | 16378985 |
| **MG505.e1** | NBT[a] | M-F[c] | A | R5 | Chronic | NC | 17/46 | 27 | ABA61511.1 | 16378985 |
| **BF520.e3** | NBT[a] | MTCT[b] | A | R5 | Acute | 2 | 17/41 | 28 | KX168096 | 27345369 |
| **BS208.b1** | NBT[a] | MTCT[b] | A | R5 | Acute | 2 | 13/42 | 22 | KX364401 | 16378985 |
| **PVO.4** | Italy | M-M[d] | B | R5 | Acute | 2/3 | 29/48 | 32 | AAW64259.1 | 16051804 |
| **KNH1144** | Discarded blood units from Kenyatta National Hospital | Unknown | A | R5 | Chronic | NC[f] | 28/44 | 27 | AAN03143.1 | 12218394 |

[a]Nairobi Breast Feeding Clinical Trial
[b]Mother-to-child-transmission
[c]Male to female transmission
[d]Male to male transmission
[e]Predicted using Los Alamos HIV sequence database N-GlycoSite software
[f]Not characterized

**Table 2. Dynamic light scattering measurements of trimer dimensions, purity and thermal stability.**

| Env | Radius (nm) [a] | Polydispersity (%) | MW-R (KDa) [b] | Onset of Melting (°C) |
|---|---|---|---|---|
| BG505.c2 | 6.66 | 5.01 | 284.47 | 64 |
| PVO.4 | 6.63 | 6.23 | 281.6 | 60.3 (3 mg/mL) |
| BF520.e3 | 6.74 | 4.27 | 292.8 | 63.3 |
| BS208.b1 | 6.49 | 3.38 | 268.1 | 68.4 (onset of aggregation 84.7) |
| KNH1144 | 6.69 | 4.7 | 287 | 62.6 |
| KNH1144 A162T | 6.81 | 3.9 | 300 | 65.8 |
| MG505.e1 | 6.83 | 2.74 | 301.95 | 65.3 |

[a]Hydrodynamic radius (Rh)
[b]The molar mass derived DLS estimates of size, density, and particle conformation

HEK293F Supernatant

(FIG 2)

Galanthus *nivalis* Lectin Affinity

(FIG 3A)

DEAE Anion-Exchange (IEX)

(FIG 3B)

Hydrophobic Interaction (HIC)

(FIG 4)

Size Exclusion Chromatography (SEC)

Analytical SEC

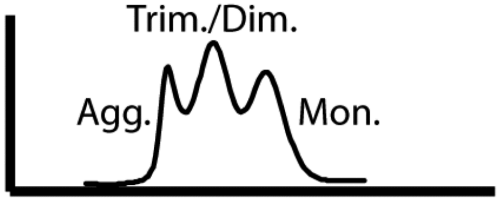


Anion-Exchange

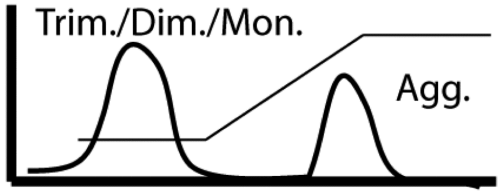


HIC

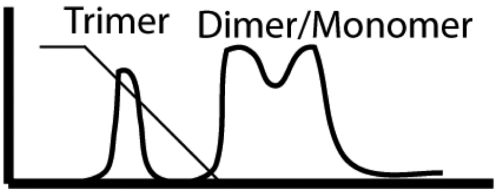


SEC